

# Proteomic Mechanisms of Cardioprotection during Mammalian Hibernation in Woodchucks, *Marmota Monax*

Hong Li,<sup>\*,†</sup> Tong Liu,<sup>†</sup> Wei Chen,<sup>†</sup> Mohit Raja Jain,<sup>†</sup> Dorothy E. Vatner,<sup>‡</sup> Stephen F. Vatner,<sup>‡</sup> Raymond K. Kudej,<sup>‡</sup> and Lin Yan<sup>\*,‡</sup>

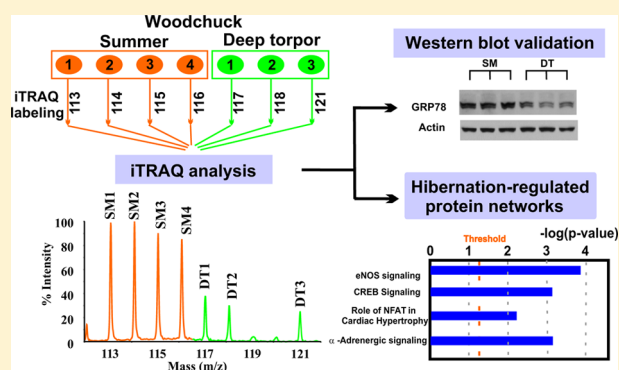
<sup>†</sup>Center for Advanced Proteomics Research and Department of Biochemistry and Molecular Biology, Rutgers University-New Jersey Medical School Cancer Center, Newark, New Jersey 07103, United States

<sup>‡</sup>Cardiovascular Research Institute and Department of Cell Biology and Molecular Medicine, Rutgers University-New Jersey Medical School, Newark, New Jersey 07103, United States

## S Supporting Information

**ABSTRACT:** Mammalian hibernation is a unique strategy for winter survival in response to limited food supply and harsh climate, which includes resistance to cardiac arrhythmias. We previously found that hibernating woodchucks (*Marmota monax*) exhibit natural resistance to Ca<sup>2+</sup> overload-related cardiac dysfunction and nitric oxide (NO)-dependent vasodilation, which maintains myocardial blood flow during hibernation. Since the cellular/molecular mechanisms mediating the protection are less clear, the goal of this study was to investigate changes in the heart proteome and reveal related signaling networks that are involved in establishing cardioprotection in woodchucks during hibernation. This was accomplished using isobaric tags for a relative and absolute quantification (iTRAQ) approach. The most significant changes observed in winter hibernation compared to summer non-hibernation animals were upregulation of the antioxidant catalase and inhibition of endoplasmic reticulum (ER) stress response by downregulation of GRP78, mechanisms which could be responsible for the adaptation and protection in hibernating animals. Furthermore, protein networks pertaining to NO signaling, acute phase response, CREB and NFAT transcriptional regulations, protein kinase A and  $\alpha$ -adrenergic signaling were also dramatically upregulated during hibernation. These adaptive mechanisms in hibernators may provide new directions to protect myocardium of non-hibernating animals, especially humans, from cardiac dysfunction induced by hypothermic stress and myocardial ischemia.

**KEYWORDS:** iTRAQ, true hibernation, cardioprotection



summer non-hibernation animals were upregulation of the antioxidant catalase and inhibition of endoplasmic reticulum (ER) stress response by downregulation of GRP78, mechanisms which could be responsible for the adaptation and protection in hibernating animals. Furthermore, protein networks pertaining to NO signaling, acute phase response, CREB and NFAT transcriptional regulations, protein kinase A and  $\alpha$ -adrenergic signaling were also dramatically upregulated during hibernation. These adaptive mechanisms in hibernators may provide new directions to protect myocardium of non-hibernating animals, especially humans, from cardiac dysfunction induced by hypothermic stress and myocardial ischemia.

## INTRODUCTION

Mammalian hibernation is an energy-conservation strategy that allows various small animals to survive winter under conditions of low temperatures and food scarcity. Hibernators such as woodchucks undergo a remarkable phenotypic switch that involves physiological, morphological, and biochemical changes in response to environmental stresses.<sup>1</sup> During hibernation, hibernators sink into deep torpor (DT) where the metabolic rate is below 5% of the normal rate, body temperature typically falls to 32–50 °F, and physiological functions, as well as protein turnover, are profoundly depressed. During DT, to match decreased metabolic demand, heart rate, mean arterial pressure, and maximum and minimum left ventricle (LV) pressure change rates ( $dP/dt$ ) are significantly decreased in woodchucks.<sup>2</sup> However, myocardial blood flow is actually maintained, which is in apparent contradiction to the concept of decreased myocardial blood flow matching reduced metabolic demand.<sup>2</sup> Major cardiac stress adaptation during hibernation includes resistance to fibrillation/arrhythmias,<sup>3</sup> dynamic main-

tenance of conduction and repolarization patterns through improved gap junction functions,<sup>4</sup> maintenance of Na<sup>+</sup>/K<sup>+</sup> ion homeostasis<sup>5</sup> and improved Ca<sup>2+</sup> handling.<sup>6</sup> Despite the dramatic physiological adaptation to harsh environment during hibernation, the molecular basis for the adaptive mechanisms in hibernating animals is not well-known. We have previously observed that woodchucks demonstrate epigenetic changes from summer to winter in response to ischemic injury.<sup>7,8</sup> Although there is now a considerable amount of information related to various aspects of the morphological, physiological, and biochemical changes that are associated with the dramatic adaptation of hibernating myocardium,<sup>2–6</sup> the cellular and molecular basis of mammalian hibernation, especially in cardioprotection, are still poorly understood. It is likely that novel mechanisms are involved in cardioprotection but are not yet identified.

Received: June 18, 2013

Published: July 12, 2013

Proteomics approaches are effective at identifying new protein signaling networks, which cannot be readily identified with targeted biochemical approaches. Using a label-free approach, Shao et al. discovered that proteins involved in translation, protein turnover, mRNA processing, and oxidative phosphorylation significantly changed in the livers of ground squirrels (*Urocyon parryi*) throughout the torpor–arousal cycle during hibernation.<sup>9</sup> In contrast, Martin et al. used the two-dimensional differential gel electrophoresis approach to identify protein differences in the intestines of ground squirrels (*Ictidomys tridecemlineatus*) between sham-treated animals with those exposed to ischemia-reperfusion (I/R);<sup>10</sup> these proteomics profiles of intestines were able to distinguish among the sham-treated summer and hibernating samples, as well as I/R-induced proteomic changes between summer and hibernating animals. More recently Grabek et al. discovered the importance of proteins involved in ATP-conserving mechanisms for winter cardioprotection in the hearts of 13-lined ground squirrels.<sup>11</sup> In the present study, we conducted iTRAQ quantitative proteomics experiments in order to discover hibernation specific cardiac proteomic changes in *Marmota monax*; the sample set involved winter animals in DT and the summer (SM) non-hibernating animals. Because the woodchuck is not a widely studied animal model, a complete set of gene and protein sequences is not yet available. Although the availability of high resolution tandem mass spectrometers has enabled the acquisition of high resolution MS/MS spectra, software packages for high-throughput “deep” *de novo* sequencing of shotgun proteomics data and subsequent assembly of peptides into protein sequences are not yet robust enough for routine shotgun proteomics studies of rare species. Consequently, we designed the iTRAQ proteomics approach to search the MS/MS spectra obtained from woodchuck peptides against both rodent and human protein sequences and quantified over 4,000 unique proteins. Based on these quantitative proteomics studies, a surprisingly small number of protein networks are altered during DT, suggesting that a select scope of mechanisms may be important for determining cardiac protection in hibernating animals. Development of therapeutics that can recapitulate protein signaling networks similar to the ones found in hibernating animals may lead to better treatments of vascular human diseases.

## MATERIALS AND METHODS

### Reagents

All chemical reagents were purchased from Sigma (St. Louis, MO) unless otherwise indicated. Sequencing grade trypsin, triethylammonium bicarbonate (TEAB), NP-40, Triton X-100, protease inhibitor cocktail, phosphatase inhibitor cocktail, phosphate buffer saline (PBS),  $\text{KH}_2\text{PO}_4$ , KCl, formic acid (FA), BCA protein assay kit were purchased from Thermo Scientific (Rockford, IL). iTRAQ 8-plex kit containing tris(2-carboxyethyl) phosphine (TCEP), methyl methanethiosulfonate (MMTS), and 8-plex iTRAQ reagents were obtained from AB SCIEX (Foster City, CA). Acetonitrile (ACN) and HPLC-grade water were purchased from J. T. Baker (Phillipsburg, NJ).

### Animal Models

Animals used in this study were maintained in accordance with the *Guide for the Care and Use of Laboratory Animals* (National Research Council, Eighth Edition) and the Institutional Animal Care and Use Committee at Rutgers-New Jersey Medical School. Woodchucks used in this study were obtained from

Northeastern Wildlife, Idaho. The following groups of animals were analyzed in this study: DT Group: During winter in Dec–Jan, a group of the male and female woodchucks ( $n = 3$  or 4 were used for different experiments due to limited availability of this animal model) was instrumented (see Supporting Information and Methods for details) for telemetry (model d70-pctp, Data Science International (DSI), St. Paul, MN) and LV pressure measurements using a micromanometer (Konigsberg Instruments, Inc., Pasadena, CA). After 2 weeks of recovery, the woodchucks were placed in the hibernaculum (40–42 °F) (see Supporting Information and Methods) without food to allow the animals to go into DT. The animals were monitored for electrocardiography (ECG or EKG) via a telemetry system with d70-pctp as a transmitter and rmc-1 as a DSI receiver. After the animals demonstrated a prolonged DT (heart rate < 25 bpm for 2 days and no response to mild external stimuli), the animals were performed for either physiological analysis or euthanized with sodium pentobarbital (100 mg/kg, iv to effect) for heart tissue collection. SM Group: As the base comparison group for the iTRAQ study, heart samples were collected from woodchucks in summer (SM, June–July,  $n = 3–5$ ) for both iTRAQ proteomics and downstream biochemical studies described in this study. After the hearts were excised, the blood was quickly washed out from the heart with saline, and the tissue samples were frozen at  $-80$  °C prior to analysis.

### Protein Extraction and iTRAQ Labeling

One set of 8-plex iTRAQ reagents was used for labeling 7 samples in the experiment (see experimental design in Supplemental Table 1). The hearts were first rinsed with PBS containing a protease inhibitor cocktail on ice to remove any residual blood prior to protein extraction. Proteins were extracted from the 30 mg of heart tissue from each animal using 0.5 mL of lysis buffer containing 100 mM TEAB, 1% NP40, 1% Triton X-100, a protease inhibitor cocktail and a phosphatase inhibitor cocktail. BCA protein assay was used for protein concentration measurements. Following the manufacturer’s instructions (AB SCIEX), 100  $\mu\text{g}$  of protein from each sample was first reduced by 5 mM TCEP at 60 °C for 1 h, then alkylated with 10 mM MMTS at RT for 10 min, followed by trypsin digestion (1:10 by weight, enzyme to protein ratio) overnight. The peptides derived from the 4 summer woodchucks (SM1 to SM4) were labeled with iTRAQ reagents 113, 114, 115, and 116, and 3 deep torpor woodchucks (DT1–DT3) were labeled with iTRAQ reagents 117, 118, and 121; iTRAQ 119 was not used due to limited availability of DT animals at the time of the experiment.

### Liquid Chromatography and Tandem Mass Spectrometry (LC–MS/MS)

The iTRAQ-labeled peptides were first combined according to the experimental design outlined in Supplemental Table 1 and were then fractionated by strong cation exchange chromatography (SCX) on a BioCAD Perfusion Chromatography System (AB SCIEX). A polysulfethyl A column (4.6 mm  $\times$  200 mm, 5  $\mu\text{m}$ , 300 Å, Poly LC Inc., Columbia, MD, USA) was used with a 1-h binary gradient consisting of mobile phase A (10 mM  $\text{KH}_2\text{PO}_4$  and 25% ACN, pH 2.7) and mobile phase B (600 mM KCl, 10 mM  $\text{KH}_2\text{PO}_4$  and 25% ACN, pH 2.7), as described previously.<sup>12</sup> For each SCX separation, 10 fractions with similar peptide complexities were collected. The peptides in the SCX fractions were desalted using PepClean C<sub>18</sub> spin columns (Pierce, Rockford, IL, USA) prior to the LC–MS/MS analysis

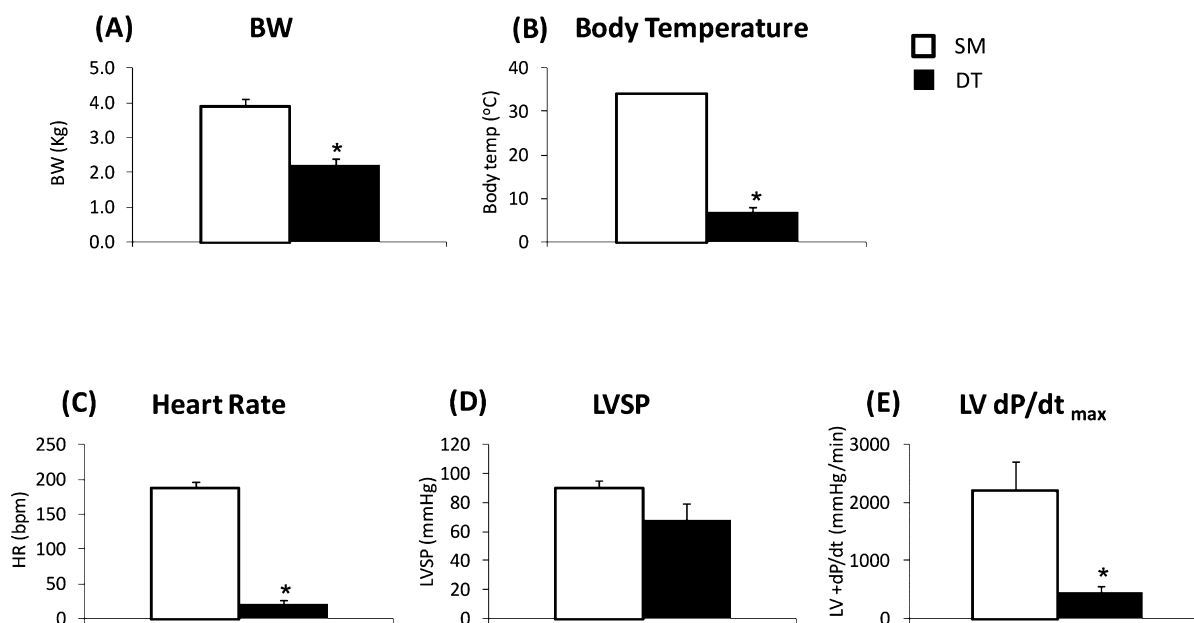


**Figure 1.** Comparison of cardiac function among woodchucks living in the summer and winter with DT. (A) Average woodchuck body weight (BW) was lower during DT. (B) The body temperature was dramatically lower during DT only. (C) The heart rate was dramatically reduced during DT. (D) DT resulted in a trend (but not significant) toward a decrease in LV systolic pressure (LVSP). (E) DT resulted in a significant decrease in maximum LV dp/dt. All measurements were performed in woodchucks in summer ( $n = 5$ ) and winter during DT ( $n = 4$ ). \* $p < 0.05$  vs summer. Data are expressed as mean  $\pm$  SEM.

by reversed phase liquid chromatography (RPLC) on an Ultimate 3000 LC system (Dionex) coupled with an LTQ Orbitrap Velos tandem mass spectrometer (Thermo Scientific). In brief, the peptides were separated by a  $C_{18}$  RPLC column ( $75 \mu\text{m} \times 150 \text{ mm}$ ,  $3 \mu\text{m}$ ,  $100 \text{ \AA}$ ,  $C_{18}$ , Dionex, Sunnyvale, CA, USA) at  $250 \text{ nL/min}$  using an 180-min gradient consisted of solvent A (2% ACN and 0.1% FA) and solvent B (85% ACN and 0.1% FA): 0–140 min, from 3% to 25% B; 140–160 min, from 25% to 45% B and 160 to 170 min, from 45% to 95% B. The eluted peptides were introduced into the Orbitrap *via* a Proxeon nano electrospray ionization source with a spray voltage of 2 kV and a capillary temperature of  $275 \text{ }^\circ\text{C}$ . MS spectra were acquired in the positive ion mode with a scanning mass range of  $m/z$  350–2,000 and a resolution of 60,000 full-width at half-maximum (fwhm). The 10 most abundant ions were selected for collision-induced dissociation (CID) fragmentation in the ion trap followed by HCD fragmentation in the Orbitrap. The normalized collision energies were set to 35 for CID and 45 for HCD. The precursor isolation width was set at 2 amu, and a minimum ion threshold count was set as 3,000. The lock mass feature was engaged for accurate mass measurements. An  $m/z$  445.120030 corresponding to polysiloxane ion was used as the lock mass for internal calibration.

#### Bioinformatics Analysis

The MS/MS spectra were searched against either a UniRef100 human (120,982 entries), mouse (82,522 entries), or rat (51,862 entries) database (downloaded on January 20, 2012), using both Mascot (V.2.3) and SEQUEST search engines *via* the Proteome Discoverer platform (V. 1.3, Thermo Scientific). The precursor mass error window was set as 10 ppm, and MS/MS error tolerance was set as 0.1 Da for HCD spectra and 0.5 Da for CID spectra with up to one missed tryptic cleavage. Methionine oxidation and tyrosine 8-plex iTRAQ labeling were set as variable modifications, whereas N-terminus and lysine side chain 8-plex iTRAQ labeling and cysteine MMTS

conjugation were set as fixed modifications. The resulting .dat files from Mascot and .msf files from Proteome Discoverer were filtered with Scaffold (V3.3.2, Proteome Software, Inc., Portland, OR) for protein identification and quantification analyses. All peptides were identified with at least 95% confidence interval value (CI value) as specified by the Peptide Prophet algorithm and less than 1% false discovery rate (FDR) based on forward/reverse database searches.<sup>13</sup> Proteins were considered confidently identified with at least one unique peptide and an experiment-wide FDR of no more than 1.5%. Proteins that share the same peptides and could not be differentiated on the basis of MS/MS analysis alone were grouped together to reduce the redundancy, using Scaffold. Relative quantification of proteins was determined with Scaffold Q+ module in a normalized  $\log_2$ -based relative iTRAQ ratio format, with iTRAQ 113 tag as the reference denominator. The average protein expression ratios between SM and DT groups were calculated as the following: (average of the three DT ratios)/(average of the four SM ratios). Significance of protein expression changes in  $p$ -values were calculated using a two-tailed Student's  $t$  test for each protein, with the three DT ratios comparing to their corresponding four SM ratios. The proteins with a greater than 20% changes and  $p$ -values  $\leq 0.05$  are considered as significantly changed based on our previously determined analytical variations.<sup>14</sup> For functional analysis of the affected protein networks, the significantly changed proteins were submitted to Ingenuity (<http://www.ingenuity.com/>) for pathway analysis.

#### Western Blotting

A  $20\text{-}\mu\text{g}$  portion of proteins/lane from each sample was separated using 10% SDS-PAGE gels and transferred onto nitrocellulose membranes (Biorad, Hercules, CA, USA), which were probed with the primary antibodies at  $4 \text{ }^\circ\text{C}$  overnight: anti-catalase (1:5000, Abcam, Cambridge, MA); anti-GRP78 (1:1000, Stressgen Bioreagents, Brussels, Belgium); anti-

Table 1. Cross-Species Database Search for the Identification of Woodchuck Cardiac Proteins

experimental design <sup>a</sup>	human			mouse			rat		
	protein	peptide	FDR	protein	peptide	FDR	protein	peptide	FDR
DT vs SM	4,293	8,742	0.5%	4,226	8,608	1.4%	4,381	8,530	1.3%

<sup>a</sup>The raw spectra from the iTRAQ analysis were independently searched against human, mouse, and rat sequences in the UniRef 100 database, using the search results combined from Mascot (v2.3) and Sequest search engines through the Proteome Discoverer software (v1.3). The resulting files were imported into Scaffold for both qualitative and quantitative analyses. The number of proteins and peptides identified from each database search are listed in this table, following stringent data filtering described in Materials and Methods.

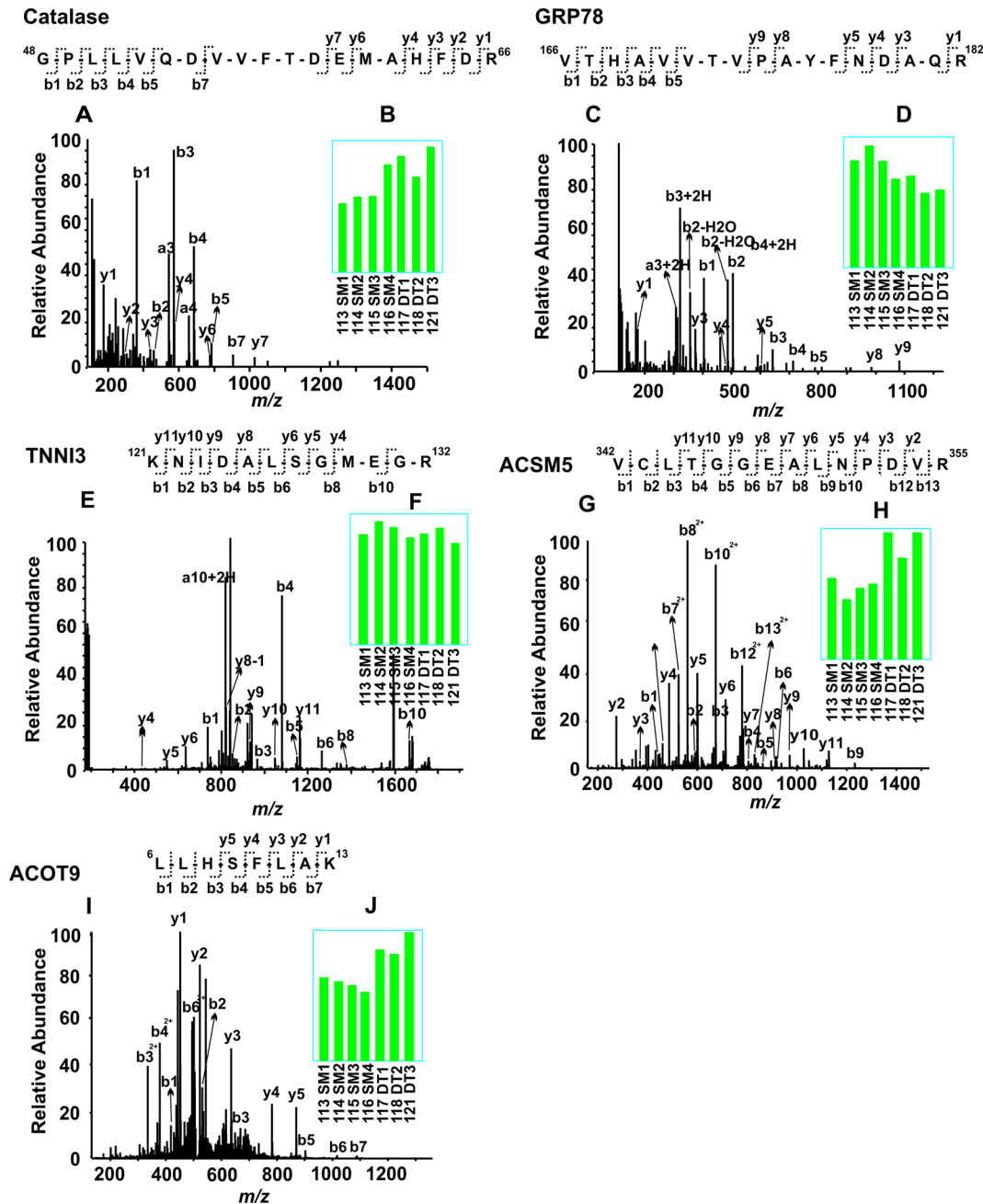


**Figure 2.** Example of iTRAQ analyses of woodchuck cardiac proteomic changes among SM and DT animal groups. MS/MS spectra (A, C, E, G, and I) enabled confident identifications of peptide sequences based on the determination of stretches of continuous series of y ions and b ions. The bar graph inserts (B, D, F, H, and J) indicate the normalized intensities of the iTRAQ tags observed in each MS/MS spectrum. Compared to SM, catalase was upregulated in the DT group, whereas 78 kDa glucose-regulated protein (GRP78) was downregulated. Troponin I type 3 (TNNI3) did not change. Both acyl-coenzyme A synthetase (ACSM5) and acyl-coenzyme A thioesterase 9 (ACOT9) were upregulated in the DT group.

Troponin I (1:1000, Fitzgerald, Acton, MA); anti-ATM (1:2000, Sigma-Aldrich, St Louis, MO); anti-PI3 Kinase

p110 $\alpha$  (1:1000, Cell Signaling, Danvers, MA); anti-PI3 Kinase p85 (1:1000, Cell Signaling); anti-PKA 2 $\beta$  (1:1000, Abcam);

anti-Protein Kinase A regulatory I $\alpha$  (1:1000, Abcam); anti-AKAP2 (1:500, Assay Biotechnology, Sunnyvale, CA); anti-CaMKII (1:500, Abcam); anti- $\beta$ -catenin ES (1:500, Santa Cruz, Santa Cruz, CA), and anti-actin (Santa Cruz). Secondary antibodies, including a goat anti-rabbit IgG (1:5000, Biorad) or a goat anti-mouse IgG (1:5000, Biorad) were used for the visualization of the membrane with enhanced chemiluminescent substrate (PerkinElmer, Waltham, MA).

## RESULTS AND DISCUSSION

### Hibernating Animals Have Unique Cardiac Physiology

Physiological and hemodynamic data indicate that hibernating woodchucks entering DT have a distinct cardiac functional profile compared to the animals analyzed in summer (SM) (Figure 1). As expected, the body weights (BW) were significantly lower in woodchucks in winter DT, when compared to summer (Figure 1A). Both body temperatures and heart rates were dramatically reduced in DT (Figure 1B and C). Physiologically, DT resulted in a trend, albeit insignificant, decrease in left ventricle (LV) systolic pressure (LVSP, Figure 1D); on the other hand, DT caused a significant decrease in maximum LV pressure change rate,  $dp/dt$  (Figure 1E). These data correlated well with the notion that the woodchucks exhibit a suppression of LV systolic function to match decreased metabolic demand during winter particularly when they enter the phase of torpor.

### Cross-Species Database Searches Can Effectively Identify Woodchuck Proteins

In order to discover proteomic changes in hibernating woodchucks, we conducted iTRAQ analyses to identify seasonal proteomic changes by comparing the differentially expressed proteins between DT vs SM (Supplemental Table 1). Since a comprehensive protein database for woodchucks is not available, we used a cross-species database search strategy for the identification of woodchuck proteins. For each set of iTRAQ experiments, the MS/MS spectra were searched independently against either the UniRef100 human (120,982 sequences), mouse (82,522 sequences), or rat (51,862 sequences) database. Positive protein identifications were based on the forward/reverse sequence database search routine, filtered at the protein FDR  $\leq 1.5\%$  via Scaffold. Each identified protein contains at least one unique peptide with a CI value  $\geq 95\%$ . Despite the vast differences in the sequence database sizes, similar numbers of proteins were identified across the three species, ranging from low to mid 4,000s (Table 1, Supplemental Tables 2A; also provided to the readers are proteins identified with at least two peptides, Supplemental Tables 2B), while slightly more unique peptides were identified using the human relative to rodent databases. It appeared that these protein sequences are conserved between woodchucks and either human, mouse, or rat proteins to render this cross-species database search strategy effective.

### Identification of Torpor-Specific Proteomic Changes

Based on our previous analysis of iTRAQ analytical variation<sup>14</sup> on our instruments, the proteins with iTRAQ ratios beyond 20% of the normalized population means and  $p$ -values  $\leq 0.05$  are considered as significantly changed. Consequently, we found 162 proteins in DT vs SM (Supplemental Table 3A) were significantly changed (also provided to the readers are more confidently identified proteins, with at least two matched peptides, Supplemental Tables 3B). Given the dramatic cardiac

functional changes that occur during DT, it is surprising that less than 5% of the identified proteins were significantly altered in DT animals, suggesting the importance of key protein networks in determining cardiac protective mechanisms during DT.

Evaluation of representative MS/MS spectra confirmed DT-specific alternation of proteins (Figure 2). For example, both catalase and 78 kDa glucose-regulated protein (GRP78) were altered in DT compared to summer, with the expression levels of catalase increased (Figure 2A and B) and GRP78 decreased (Figure 2C and D). In contrast, like most identified proteins, troponin I type 3 (TNNI3) was not altered by DT (Figure 2, E and F). Lipid metabolic enzymes, acyl-coenzyme A synthetase medium-chain family member 5 (ACSM5), and mitochondrial acyl-coenzyme A thioesterase 9 (ACOT9) were also elevated during DT (Figure 2G–J). It is clear from the iTRAQ experiments that the availability of the 8-plex iTRAQ reagents for incorporating relatively large numbers of animal samples in each multiplexing expression profiling experiment is crucial for discovering significant proteomics changes, since the random variations among different animals are unavoidable. Furthermore, validation of key protein expression changes by alternative, largely antibody-based approaches is also important for understanding the biological significance of the protein networks affected.

### Validation of iTRAQ-Derived Changes by Western Blotting

Following iTRAQ analyses, we performed additional Western blotting in order to verify key proteomic differences discovered by iTRAQ analyses. Similar to the discovery made with iTRAQ analysis when compared to the summer group, the upregulation of antioxidant catalase and the downregulation of ER stress regulator GRP78 were occurring in DT (Figure 3A and B). Overexpression of catalase and inhibition of ER stress response by downregulation of GRP78 have been reported to be involved in cardioprotection.<sup>15–21</sup>

We also confirmed the significant changes of key signaling protein networks in DT over SM, including the increase of ataxia telangiectasia mutated protein (ATM), the regulatory subunit 2 of phosphoinositide-3-kinase (PI3KR2), A-kinase anchor protein 2 (AKAP2), cAMP-dependent protein kinase type I $\alpha$  (PRKAR1A) and II $\beta$  (PRKAR2B), and cAMP-dependent protein kinase catalytic  $\alpha$  (PRKACA) (Figure 3C and D). PI3K is a well-known kinase that regulates cell survival, growth, cell cycle entry, and cell migration through modulating its downstream targets.<sup>22</sup> The downstream targets including Akt, PKC, p70S6K, and ERK have been demonstrated to play roles in mediating cardioprotection and limiting myocardial damage induced by ischemia.<sup>22–24</sup> In addition, since hibernating animals induce adaptive cardiac hypertrophy due to increased heart contractility during DT,<sup>25,26</sup> the proteins that regulate hypertrophy could be upregulated. PI3K/AKT, p70S6K, and ERK are well-known molecules for mediating physiological hypertrophy;<sup>27–29</sup> therefore, the upregulation of PI3K-related protein networks likely contributes to enhanced cardiac hypertrophic response during DT. Cyclic AMP-dependent protein kinase (PKA) is the main mediator of cAMP signaling in mammals.<sup>30</sup> PKA induces a signal transduction through phosphorylation of different target proteins involved in the regulation of metabolism, cell proliferation, differentiation, and apoptosis. To date, four major R subunit isoforms (RI $\alpha$ , RI $\beta$ , RII $\alpha$ , and RII $\beta$ ) and three isoforms of the C subunit, (C $\alpha$ , C $\beta$ , and C $\gamma$ ) have been

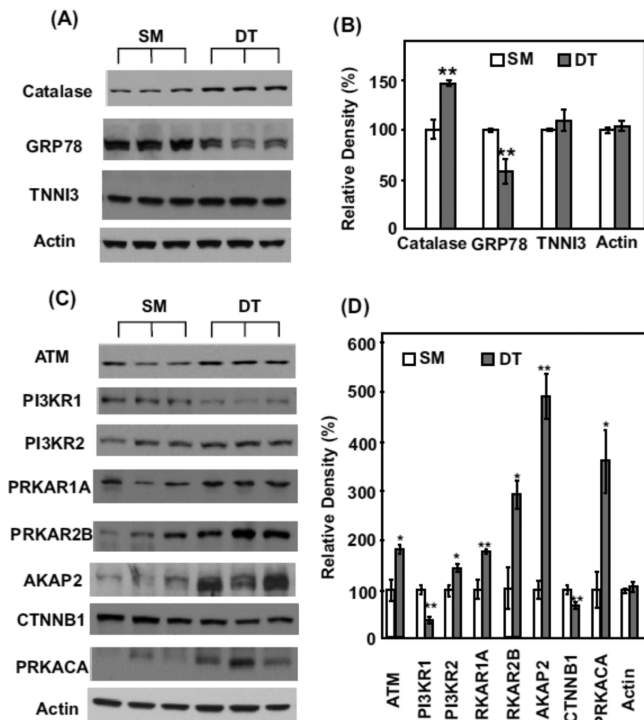


**Figure 3.** Western blot validation of iTRAQ proteomics changes among select proteins. (A) Each lane represents the proteins extracted from the heart of a single distinct woodchuck. Three samples each from SM and DT groups are blotted with the antibodies against catalase, GRP78, troponin I (TNNI3), and actin (as the loading controls), respectively. (B) The blot densities of catalase, GRP78, TNNI3, and actin were determined using Quantity One software (Bio-Rad). (C) Western blots and (D) blot densities determined by Quantity One for ATM, PI3KR1, PI3KR2, PRKAR1, PRKAR2B, AKAP2, CTNNB1, PRKACA, and actin are shown. (D) All densities were normalized to SM1 intensities for each protein for the statistical analysis. Significant expression difference from SM were determined by Student's *t* tests. \**p* < 0.05 and \*\**p* < 0.02. Data are expressed as mean (SD).

identified with distinct tissue distribution and biological features.<sup>31–33</sup> The specificity of PKA signal transduction is also mediated by compartmentalization of the isoforms through interaction with A kinase anchoring proteins (AKAPs).<sup>34</sup> Interestingly, the current study demonstrates the upregulation of AKAP2 and selective isoforms of PKA, i.e., PRKAR1A, PRKAR2B, and PRKACA, suggesting AKAP2 could interact with these PKA isoforms and target them to specific microdomains which induce specific cellular and molecular signal responses during hibernation.

#### Identification of Hibernation-Regulated Protein Networks

In order to discover novel protein networks that are regulated during hibernation, we performed a bioinformatics analysis of the significantly changed proteins from the iTRAQ analyses. Similar to the elegant work published by Russeth et al.,<sup>35</sup> it is essential to use multiple protein database search engines to achieve a broad proteome coverage for the analysis of nonmodel organisms. However, despite the recent advancements in mass spectrometry sensitivities, proteomics approaches, including the current study, still cannot match the depths of genomics studies for revealing expression changes of many low abundance molecules during hibernation.<sup>36,37</sup> It is likely that, with more high quality nucleic acid sequence data

obtained from deep sequencing studies and the improvement in bioinformatics technologies, proteomics methods can achieve much higher proteome coverages in the near future, by directly searching the MS/MS spectra against proteins predicted from deep sequencing approaches.

Despite these limitations, our study has both confirmed previous findings and revealed some novel insights regarding the effect of hibernation on protein networks. Not surprisingly, some of the protein networks affected by hibernation discovered from this study (see examples in Supplemental Table 4) have been reported previously. For example, downregulation of fatty acid synthesis and upregulation of fatty acid catabolism during hibernation have been reported from previous proteomics and genomics studies of the tissues of hibernating arctic ground squirrels<sup>9,38</sup> and also from another proteomics study of the hearts of ground squirrels.<sup>11</sup>

Interestingly, it appeared that protein networks pertaining to NO signaling, acute phase response, cAMP response element-binding protein (CREB) and nuclear factor of activated T cells (NFAT) transcriptional regulations, protein kinase A (PKA) signaling, and  $\alpha$ -adrenergic signaling were dramatically altered during DT (Figure 4A and Supplemental Table 4). A beneficial role for NO during ischemia has been clearly demonstrated.<sup>2,39–41</sup> We previously found that during DT, the myocardial blood flow was surprisingly maintained, although the blood flow to the visceral organs, e.g., to the kidneys, was decreased.<sup>2</sup> The maintenance of myocardial blood flow was apparently involved in NO-dependent vasodilation.<sup>2</sup> However, we do not know which NO synthase isoform mediates these effects in previous observations. Interestingly, in the current study, we found that endothelial nitric oxide synthase (eNOS) signaling was upregulated during DT (Figure 4A and B). eNOS has been demonstrated to mediate vasodilation and angiogenesis, which are important cardioprotective mechanisms.<sup>42–44</sup> According to the analysis of NO protein signaling networks during DT (Figure 4B), we hypothesize that NO is produced in the cardiovascular system by eNOS, following agonist induction of intracellular  $[Ca^{2+}]$  and downstream caveolin-eNOS protein complex formation.

In addition, from the network analysis, selective downstream protein network changes in DT animals suggested that CREB protein network activation may be important for cardiac protection during torpor. Several *in vitro* studies have also shown the roles of CREB in the regulation of cardiac function. In one study, the hypertrophic agonist phenylephrine promotes phosphorylation of CREB in adult rat cardiac myocytes through  $\alpha$ - and  $\beta$ -adrenergic receptors, which plays an important role in the hypertrophic response.<sup>45</sup> Another study indicates that preconditioning stimulated the induction of thioredoxin. Subsequently, thioredoxin can be translocated into the nucleus and activates CREB via phosphorylation for a delayed induction of mitochondrial antiapoptotic Bcl-2 and antioxidative MnSOD.<sup>46</sup> A more mechanistic study demonstrates that the cardioprotection induced by pharmacological preconditioning with resveratrol is mediated by the activation of CREB through the adenosine A3 receptor by Akt-dependent (PI3K-Akt-CREB-Bcl2) and Akt-independent (ERK/p38MAPK-MSK1-CREB-Bcl2) pathways.<sup>47–49</sup> Moreover, a recent study demonstrated that CREB activation mediates ischemic preconditioning.<sup>50</sup> Thus, CREB protein network activation could be involved in cardiac hypertrophy and ischemic preconditioning in hibernating animals in winter.

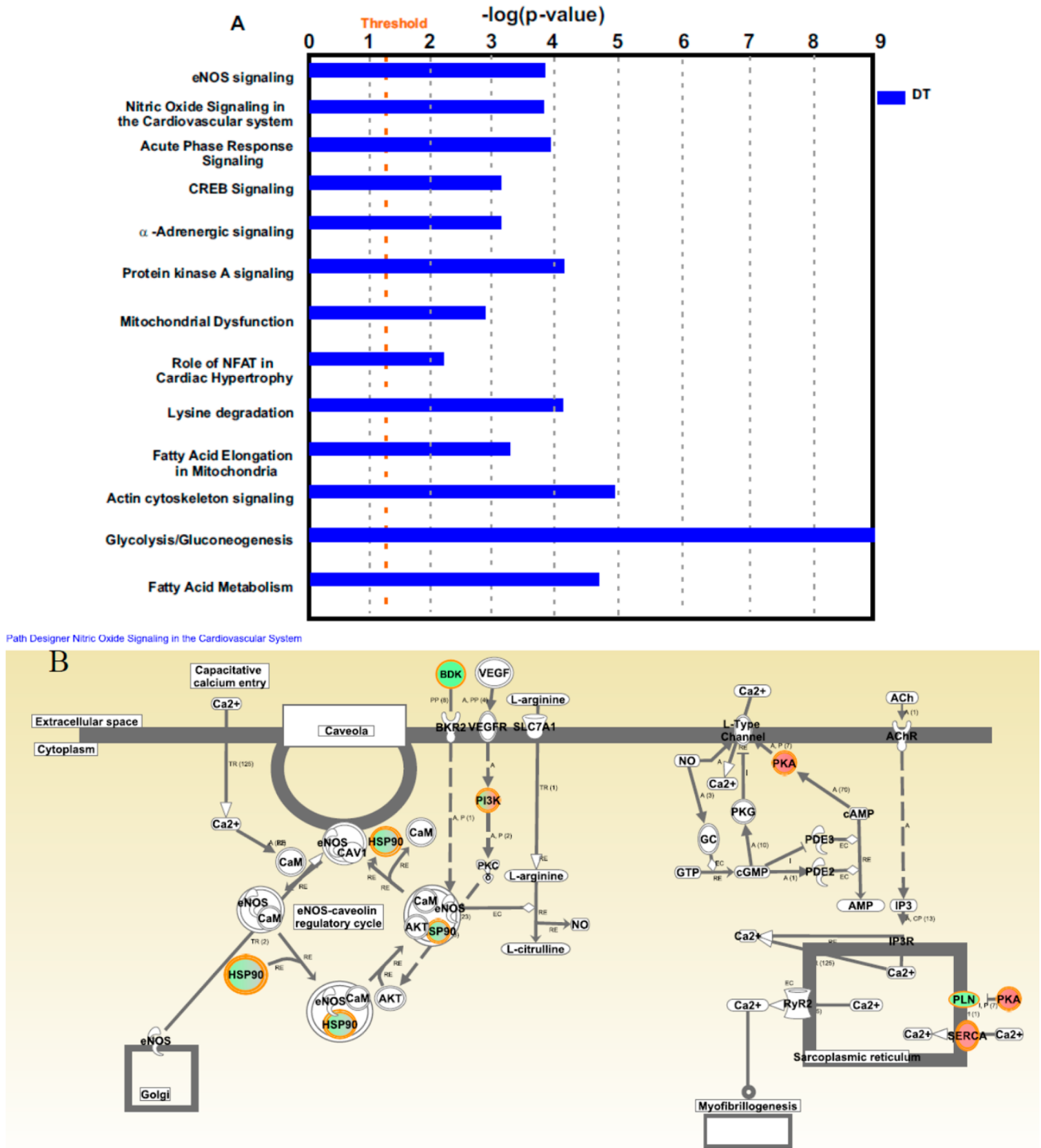


**Figure 4.** Identification of distinctive protein signaling networks modulated during DT. (A) Significantly altered protein networks from DT/SM (blue) experiments. The significantly changed proteins ( $p$ -values  $< 0.05$ ) were analyzed by Ingenuity Pathways Analysis software (IPA; Ingenuity Systems, Mountain View, CA; www.ingenuity.com). Canonical pathways that contain well-characterized metabolic and cell signaling pathways were extracted from the IPA Knowledge base (Supplemental Table 4).  $-\log_{10}(p\text{-values})$  are plotted in the x-axis. Select protein networks are shown on the y-axis. The threshold (orange line) indicates the  $p$ -value of 0.05, above which values indicate significant enrichment of protein networks. (B) Modulation of nitric oxide (NO) protein signaling networks in DT. NO is produced in the cardiovascular system by endothelial nitric oxide synthase (eNOS), following agonist induction of intracellular  $[Ca^{2+}]$  and downstream caveolin-eNOS protein complex formation. Other proteins in this network include HSP90, Akt, and CaM. Cardiac NO regulates targets such as the L-type  $Ca^{2+}$  channels via cGMP-dependent protein kinase (PKG), the cGMP-stimulated phosphodiesterase (PDE2), and the cGMP-inhibited PDE3. There is also evidence that NO may modulate the function of the ryanodine receptor  $Ca^{2+}$  release channel (RyR2). Proteins identified in this study are shown in red (increased over summer), green (downregulated from summer), or green-filled circle with red border (different isoforms with opposite regulation).

## ■ CONCLUSIONS

Hibernating mammals are models with natural myocardial protection, which can provide mechanisms involved in cardioprotection. Proteomics analysis demonstrated that hibernating woodchucks may “prepare” for winter by evoking their intrinsic cardioprotective proteomic mechanisms, which include upregulation of the antioxidant catalase and inhibition of ER stress response by downregulation of GRP78, as well as selective activation of NO signaling, acute phase response CREB and NFAT transcriptional regulation, protein kinase A and  $\alpha$ -adrenergic signaling networks for cardiac cell survival during torpor. These cellular and molecular mechanisms involved in natural resistance to cardiac stress in hibernating mammals potentially provide new strategies to protect myocardium of non-hibernating animals, especially humans, from cardiac dysfunction induced by hypothermic stress and myocardial ischemia.

## ■ ASSOCIATED CONTENT

### 📄 Supporting Information

iTRAQ experimental design; all proteins identified in SM vs DT experiment; all identified proteins in SM vs DT with at least 2 unique peptides identified from each protein; significant protein expression difference between SM and DT groups; significant protein expression difference between SM and DT groups with at least 2 unique peptides identified from each protein; and select enriched protein network by IPA in DT/SM. This material is available free of charge via the Internet at <http://pubs.acs.org>.

## ■ AUTHOR INFORMATION

### Corresponding Author

\*(H.L.) Tel: 973-972-8396, Fax: 973-972-5594, E-mail: [liho2@njms.rutgers.edu](mailto:liho2@njms.rutgers.edu). (L.Y.) Tel: 973-972-1658, Fax: 973-972-7489, E-mail: [yanl2@njms.rutgers.edu](mailto:yanl2@njms.rutgers.edu).

### Author Contributions

L.Y. and H.L. designed the experiments. S.F.V. advised on the design of woodchuck grant proposal and study. D.E.V. revised the manuscript. H.L., T.L., W.C., M.J., R.K.K., and L.Y. performed the experiments and analyzed the data.

### Notes

The authors declare no competing financial interest.

## ■ ACKNOWLEDGMENTS

The Orbitrap mass spectrometer used in this study is supported in part by NIH grant NS046593 to H.L. for the support of a Rutgers Neuroproteomics Core Facility, and L.Y. is supported by NIH grant 1R01HL091781-01.

## ■ ABBREVIATIONS

BW, body weight; CI value, confidence interval value;  $(dp/dt)$ , rate of left ventricular pressure change; DT, woodchucks in winter at low temperature with deep torpor; ECG, electrocardiography; FA, formic acid; FDR, false discovery rate; fwhm, full-width at half-maximum; HCD, higher energy collision dissociation; I/R, ischemic reperfusion; iTRAQ, isobaric tags for relative and absolute quantification; LV, left ventricle; MMTS, methyl methanethiosulfonate; MS/MS, tandem mass spectrometry; NO, nitric oxide; RPLC, reversed phase liquid chromatography; SCX, strong cation exchange; SM, woodchucks in summer; TCEP, tris(2-carboxyethyl) phosphine

## ■ REFERENCES

- (1) Carey, H. V.; Andrews, M. T.; Martin, S. L. Mammalian hibernation: cellular and molecular responses to depressed metabolism and low temperature. *Physiol. Rev.* **2003**, *83* (4), 1153–81.
- (2) Kudej, R. K.; Vatner, S. F. Nitric oxide-dependent vasodilation maintains blood flow in true hibernating myocardium. *J. Mol. Cell. Cardiol.* **2003**, *35* (8), 931–5.
- (3) Johansson, B. W. The hibernator heart—nature’s model of resistance to ventricular fibrillation. *Cardiovasc. Res.* **1996**, *31* (5), 826–32.
- (4) Fedorov, V. V.; Glukhov, A. V.; Sudharshan, S.; Egorov, Y.; Rosenshtraukh, L. V.; Efimov, I. R. Electrophysiological mechanisms of antiarrhythmic protection during hypothermia in winter hibernating versus nonhibernating mammals. *Heart Rhythm* **2008**, *5* (11), 1587–96.
- (5) Kamm, K. E.; Zatzman, M. L.; Jones, A. W.; South, F. E. Maintenance of ion concentration gradients in the cold in aorta from rat and ground squirrel. *Am. J. Physiol.* **1979**, *237* (1), C17–22.
- (6) Yatani, A.; Kim, S. J.; Kudej, R. K.; Wang, Q.; Depre, C.; Irie, K.; Kranias, E. G.; Vatner, S. F.; Vatner, D. E. Insights into cardioprotection obtained from study of cellular Ca<sup>2+</sup> handling in myocardium of true hibernating mammals. *Am. J. Physiol. Heart Circ. Physiol.* **2004**, *286* (6), H2219–28.
- (7) Peppas, A. P.; Yan, L.; T., S. Y.; Vatner, D. E.; Vatner, S. F.; Kudej, R. K. Seasonal variation in ischemia tolerance in a true mammalian hibernator. *Circulation* **2009**, *120* (S), 846.
- (8) Xie, L. H.; Yan, L.; K., K. R.; Peppas, A. P.; Zhao, Z.; Ge, H.; Feflova, N.; You, B.; Shen, Y. T.; Vatner, D. E.; F., V. S. Arrhythmia protection insights from a hibernating animal. *Circulation* **2009**, *120* (S), 674.
- (9) Shao, C.; Liu, Y.; Ruan, H.; Li, Y.; Wang, H.; Kohl, F.; Goropashnaya, A. V.; Fedorov, V. B.; Zeng, R.; Barnes, B. M.; Yan, J. Shotgun proteomics analysis of hibernating arctic ground squirrels. *Mol. Cell. Proteomics* **2010**, *9* (2), 313–26.
- (10) Martin, S. L.; Epperson, L. E.; Rose, J. C.; Kurtz, C. C.; Ane, C.; Carey, H. V. Proteomic analysis of the winter-protected phenotype of hibernating ground squirrel intestine. *Am. J. Physiol.: Regul., Integr. Comp. Physiol.* **2008**, *295* (1), R316–28.
- (11) Grabek, K. R.; Karimpour-Fard, A.; Epperson, L. E.; Hindle, A.; Hunter, L. E.; Martin, S. L. Multistate proteomics analysis reveals novel strategies used by a hibernator to precondition the heart and conserve ATP for winter heterothermy. *Physiol. Genomics* **2011**, *43* (22), 1263–75.
- (12) Liu, T.; D’Mello, V.; Deng, L.; Hu, J.; Ricardo, M.; Pan, S.; Lu, X.; Wadsworth, S.; Siekierka, J.; Birge, R.; Li, H. A multiplexed proteomics approach to differentiate neurite outgrowth patterns. *J. Neurosci. Methods* **2006**, *158* (1), 22–9.
- (13) Ai, N.; Krasowski, M. D.; Welsh, W. J.; Ekins, S. Understanding nuclear receptors using computational methods. *Drug Discovery Today* **2009**, *14* (9–10), 486–94.
- (14) Hu, J.; Qian, J.; Borisov, O.; Pan, S.; Li, Y.; Liu, T.; Deng, L.; Wannemacher, K.; Kurnellas, M.; Patterson, C.; Elkabes, S.; Li, H. Optimized proteomic analysis of a mouse model of cerebellar dysfunction using amine-specific isobaric tags. *Proteomics* **2006**, *6* (15), 4321–34.
- (15) Turdi, S.; Han, X.; Huff, A. F.; Roe, N. D.; Hu, N.; Gao, F.; Ren, J. Cardiac-specific overexpression of catalase attenuates lipopolysaccharide-induced myocardial contractile dysfunction: role of autophagy. *Free Radic. Biol. Med.* **2012**, *53* (6), 1327–38.
- (16) Ge, W.; Zhang, Y.; Han, X.; Ren, J. Cardiac-specific overexpression of catalase attenuates paraquat-induced myocardial geometric and contractile alteration: role of ER stress. *Free Radic. Biol. Med.* **2010**, *49* (12), 2068–77.
- (17) Qin, F.; Lennon-Edwards, S.; Lancel, S.; Biolo, A.; Siwik, D. A.; Pimentel, D. R.; Dorn, G. W.; Kang, Y. J.; Colucci, W. S. Cardiac-specific overexpression of catalase identifies hydrogen peroxide-dependent and -independent phases of myocardial remodeling and prevents the progression to overt heart failure in G(alpha)q-

overexpressing transgenic mice. *Circ.: Heart Failure* **2010**, *3* (2), 306–13.

(18) Chen, Y.; Yu, A.; Saari, J. T.; Kang, Y. J. Repression of hypoxia-reoxygenation injury in the catalase-overexpressing heart of transgenic mice. *Proc. Soc. Exp. Biol. Med.* **1997**, *216* (1), 112–6.

(19) Tao, J.; Zhu, W.; Li, Y.; Xin, P.; Li, J.; Liu, M.; Redington, A. N.; Wei, M. Apelin-13 protects the heart against ischemia-reperfusion injury through inhibition of ER-dependent apoptotic pathways in a time-dependent fashion. *Am. J. Physiol. Heart Circ. Physiol.* **2011**, *301* (4), H1471–86.

(20) Terai, K.; Hiramoto, Y.; Masaki, M.; Sugiyama, S.; Kuroda, T.; Hori, M.; Kawase, I.; Hirota, H. AMP-activated protein kinase protects cardiomyocytes against hypoxic injury through attenuation of endoplasmic reticulum stress. *Mol. Cell. Biol.* **2005**, *25* (21), 9554–75.

(21) Wang, X. Y.; Yang, C. T.; Zheng, D. D.; Mo, L. Q.; Lan, A. P.; Yang, Z. L.; Hu, F.; Chen, P. X.; Liao, X. X.; Feng, J. Q. Hydrogen sulfide protects H9c2 cells against doxorubicin-induced cardiotoxicity through inhibition of endoplasmic reticulum stress. *Mol. Cell. Biochem.* **2012**, *363* (1–2), 419–26.

(22) Cantley, L. C. The phosphoinositide 3-kinase pathway. *Science* **2002**, *296* (5573), 1655–7.

(23) Ban, K.; Cooper, A. J.; Samuel, S.; Bhatti, A.; Patel, M.; Izumo, S.; Penninger, J. M.; Backx, P. H.; Oudit, G. Y.; Tsushima, R. G. Phosphatidylinositol 3-kinase gamma is a critical mediator of myocardial ischemic and adenosine-mediated preconditioning. *Circ. Res.* **2008**, *103* (6), 643–53.

(24) Ravingerova, T.; Matejikova, J.; Neckar, J.; Andelova, E.; Kolar, F. Differential role of PI3K/Akt pathway in the infarct size limitation and antiarrhythmic protection in the rat heart. *Mol. Cell. Biochem.* **2007**, *297* (1–2), 111–20.

(25) Tessier, S. N.; Storey, K. B. Myocyte enhancer factor-2 and cardiac muscle gene expression during hibernation in thirteen-lined ground squirrels. *Gene* **2012**, *501* (1), 8–16.

(26) Wickler, S. J.; Hoyt, D. F.; van Breukelen, F. Disuse atrophy in the hibernating golden-mantled ground squirrel, *Spermophilus lateralis*. *Am. J. Physiol.* **1991**, *261* (5 Pt 2), R1214–7.

(27) McMullen, J. R.; Shioi, T.; Huang, W. Y.; Zhang, L.; Tarnavski, O.; Bisping, E.; Schinke, M.; Kong, S.; Sherwood, M. C.; Brown, J.; Riggi, L.; Kang, P. M.; Izumo, S. The insulin-like growth factor 1 receptor induces physiological heart growth via the phosphoinositide 3-kinase(p110alpha) pathway. *J. Biol. Chem.* **2004**, *279* (6), 4782–93.

(28) Luo, J.; McMullen, J. R.; Sobkiw, C. L.; Zhang, L.; Dorfman, A. L.; Sherwood, M. C.; Logsdon, M. N.; Horner, J. W.; DePinho, R. A.; Izumo, S.; Cantley, L. C. Class IA phosphoinositide 3-kinase regulates heart size and physiological cardiac hypertrophy. *Mol. Cell. Biol.* **2005**, *25* (21), 9491–502.

(29) Molkentin, J. D. Calcineurin-NFAT signaling regulates the cardiac hypertrophic response in coordination with the MAPKs. *Cardiovasc. Res.* **2004**, *63* (3), 467–75.

(30) Scott, J. D. Cyclic nucleotide-dependent protein kinases. *Pharmacol. Ther.* **1991**, *50* (1), 123–45.

(31) Vetter, M. M.; Zenn, H. M.; Mendez, E.; van den Boom, H.; Herberg, F. W.; Skalhegg, B. S. The testis-specific Calpha2 subunit of PKA is kinetically indistinguishable from the common Calpha1 subunit of PKA. *BMC Biochem.* **2011**, *12*, 40.

(32) Enns, L. C.; Pettan-Brewer, C.; Ladiges, W. Protein kinase A is a target for aging and the aging heart. *Aging (Albany NY)* **2010**, *2* (4), 238–43.

(33) Soberg, K.; Jahnsen, T.; Rognes, T.; Skalhegg, B. S.; Laerdahl, J. K. Evolutionary paths of the cAMP-dependent protein kinase (PKA) catalytic subunits. *PLoS One* **2013**, *8* (4), e60935.

(34) Scott, J. D.; Santana, L. F. A-kinase anchoring proteins: getting to the heart of the matter. *Circulation* **2010**, *121* (10), 1264–71.

(35) Russeth, K. P.; Higgins, L.; Andrews, M. T. Identification of proteins from non-model organisms using mass spectrometry: application to a hibernating mammal. *J. Proteome Res.* **2006**, *5* (4), 829–39.

(36) Brauch, K. M.; Dhruv, N. D.; Hanse, E. A.; Andrews, M. T. Digital transcriptome analysis indicates adaptive mechanisms in the

heart of a hibernating mammal. *Physiol Genomics* **2005**, *23* (2), 227–34.

(37) Hampton, M.; Melvin, R. G.; Kendall, A. H.; Kirkpatrick, B. R.; Peterson, N.; Andrews, M. T. Deep sequencing the transcriptome reveals seasonal adaptive mechanisms in a hibernating mammal. *PLoS One* **2011**, *6* (10), e27021.

(38) Yan, J.; Barnes, B. M.; Kohl, F.; Marr, T. G. Modulation of gene expression in hibernating arctic ground squirrels. *Physiol. Genomics* **2008**, *32* (2), 170–81.

(39) Huang, C. H.; Vatner, S. F.; Peppas, A. P.; Yang, G.; Kudej, R. K. Cardiac nerves affect myocardial stunning through reactive oxygen and nitric oxide mechanisms. *Circ. Res.* **2003**, *93* (9), 866–73.

(40) Kim, S. J.; Ghaleh, B.; Kudej, R. K.; Huang, C. H.; Hintze, T. H.; Vatner, S. F. Delayed enhanced nitric oxide-mediated coronary vasodilation following brief ischemia and prolonged reperfusion in conscious dogs. *Circ. Res.* **1997**, *81* (1), 53–9.

(41) Kudej, R. K.; Kim, S. J.; Shen, Y. T.; Jackson, J. B.; Kudej, A. B.; Yang, G. P.; Bishop, S. P.; Vatner, S. F. Nitric oxide, an important regulator of perfusion-contraction matching in conscious pigs. *Am. J. Physiol. Heart Circ. Physiol.* **2000**, *279* (1), H451–6.

(42) Justice, J. M.; Tanner, M. A.; Myers, P. R. Endothelial cell regulation of nitric oxide production during hypoxia in coronary microvessels and epicardial arteries. *J. Cell Physiol.* **2000**, *182* (3), 359–65.

(43) Kupatt, C.; Hinkel, R.; von Bruhl, M. L.; Pohl, T.; Horstkotte, J.; Raake, P.; El Aouni, C.; Thein, E.; Dimmeler, S.; Feron, O.; Boekstegers, P. Endothelial nitric oxide synthase overexpression provides a functionally relevant angiogenic switch in hibernating pig myocardium. *J. Am. Coll. Cardiol.* **2007**, *49* (14), 1575–84.

(44) Kukreja, R. C.; Xi, L. eNOS phosphorylation: a pivotal molecular switch in vasodilation and cardioprotection? *J. Mol. Cell. Cardiol.* **2007**, *42* (2), 280–2.

(45) Markou, T.; Hadzopoulou-Cladaras, M.; Lazou, A. Phenylephrine induces activation of CREB in adult rat cardiac myocytes through MSK1 and PKA signaling pathways. *J. Mol. Cell. Cardiol.* **2004**, *37* (5), 1001–11.

(46) Chiueh, C. C.; Andoh, T.; Chock, P. B. Induction of thioredoxin and mitochondrial survival proteins mediates preconditioning-induced cardioprotection and neuroprotection. *Ann. N.Y. Acad. Sci.* **2005**, *1042*, 403–18.

(47) Das, S.; Tosaki, A.; Bagchi, D.; Maulik, N.; Das, D. K. Potentiation of a survival signal in the ischemic heart by resveratrol through p38 mitogen-activated protein kinase/mitogen- and stress-activated protein kinase 1/cAMP response element-binding protein signaling. *J. Pharmacol. Exp. Ther.* **2006**, *317* (3), 980–8.

(48) Das, S.; Tosaki, A.; Bagchi, D.; Maulik, N.; Das, D. K. Resveratrol-mediated activation of cAMP response element-binding protein through adenosine A3 receptor by Akt-dependent and -independent pathways. *J. Pharmacol. Exp. Ther.* **2005**, *314* (2), 762–9.

(49) Das, S.; Cordis, G. A.; Maulik, N.; Das, D. K. Pharmacological preconditioning with resveratrol: role of CREB-dependent Bcl-2 signaling via adenosine A3 receptor activation. *Am. J. Physiol. Heart Circ. Physiol.* **2005**, *288* (1), H328–35.

(50) Marais, E.; Genade, S.; Lochner, A. CREB activation and ischaemic preconditioning. *Cardiovasc. Drugs Ther.* **2008**, *22* (1), 3–17.